Pro-differentiating compounds for human intervertebral disc cells are present in Violina pumpkin leaf extracts

ELISABETTA LAMBERTINI[1], LETIZIA PENOLAZZI[1], MARIA PINA NOTARANGELO[1], SERENA FIORITO[2], FRANCESCO EPIFANO[2], ASSUNTA PANDOLFI[3] and ROBERTA PIVA[1]

[1]Department of Neuroscience and Rehabilitation, University of Ferrara, I-44121 Ferrara; [2]Department of Pharmacy, University 'G. D'Annunzio' of Chieti-Pescara; [3]Department of Medical, Oral and Biotechnological Sciences, Center for Advanced Studies and Technology-University G. D'Annunzio of Chieti-Pescara, I-66100 Chieti, Italy

Received December 23, 2022; Accepted February 15, 2023

DOI: 10.3892/ijmm.2023.5242

Abstract. Intervertebral disc (IVD) degeneration (IDD) is closely associated with inflammation, oxidative stress and loss of the discogenic phenotype, which current therapies are unable to reverse. In the present study, the effects of acetone extract from Violina pumpkin (*Cucurbita moschata*) leaves on degenerated IVD cells were investigated. IVD cells were isolated from the degenerated disc tissue of patients undergoing spinal surgery and were exposed to acetone extract and three major thin layer chromatography subfractions. The results revealed that, in particular, the cells benefited from exposure to subfraction Fr7, which consisted almost entirely of p-Coumaric acid. Western blot and immunocytochemical analysis showed that Fr7 induced a significant increase in discogenic transcription factors (SOX9 and tricho-rhino-phalangeal syndrome type I protein, zinc finger protein), extracellular matrix components (aggrecan, collagen type II), cellular homeostasis and stress response regulators, such as FOXO3a, nuclear factor erythroid 2-related factor 2, superoxide dismutase 2 and sirtuin 1. Two important markers related to the presence and activity of stem cells, migratory capacity and OCT4 expression, were assessed by scratch assay and western blotting, respectively, and were significantly increased in Fr7-treated cells. Moreover, Fr7 counteracted H_2O_2-triggered cell damage, preventing increases in the pro-inflammatory and anti-chondrogenic microRNA (miR), miR-221. These findings strengthen the hypothesis that adequate stimuli can support resident cells to repopulate the degenerated IVD and restart the anabolic machinery. Taken together, these data contribute to the discovery of molecules potentially effective in slowing the progression of IDD, a disease for which there is currently no effective treatment. Moreover, the use of part of a plant, the pumpkin leaves, which is usually considered a waste product in the Western world, indicated that it contains substances with potential beneficial effects on human health.

Correspondence to: Professor Roberta Piva, Department of Neuroscience and Rehabilitation, University of Ferrara, Via Fossato di Mortara 74, I-44121 Ferrara, Italy
E-mail: piv@unife.it

Key words: discogenic phenotype, intervertebral disc degeneration, p-Coumaric acid, pumpkin leaf extracts, microRNA-221

Introduction

Intervertebral disc (IVD) degeneration (IDD) is a very common multifactorial phenomenon, which causes a number of spinal-related disorders associated with heavy social costs due to the disabilities suffered by patients (1). As society ages, the incidence of IDD is on the rise and the disease has become a major global health problem in recent years (2). At present, IDD cannot be reversed by the available treatment options. Notably, interventions for IDD mainly involve the use of analgesics for pain relief, or surgical treatments that cannot be considered curative and may lead to biomechanical problems (3). The IVD is a complex articular fibrocartilaginous tissue that connects adjacent vertebral bodies to enable spinal motion (4).

In research regarding the most appropriate stimuli to suppress inflammation, oxidative stress and the catabolic processes that characterize the degenerated IVD microenvironment, there has been an increasing interest in the study of natural products of plant origin to identify novel therapeutic agents (5). The effects of numerous plant compounds, such as phenolics, flavonoids, alkaloids, terpenoids, saponins and quinones, have recently been investigated in different IDD experimental models, and in some cases, the mechanisms of action through which they influence specific signalling pathways, such as Keap1/nuclear factor erythroid 2-related factor 2 (Nrf2) or TLR4/NLRP3, have been reported (5-7).

To date, most plant extracts/herbal compounds have been evaluated for their ability to promote the synthesis of extracellular matrix (ECM) components, such as proteoglycans and type II collagen, reduce their degradation, inhibit apoptosis or senescence of IVD cells, or inhibit markers of inflammation (5). By contrast, pro-differentiating or repairing/regenerating effects remain more difficult to demonstrate. However, this is a particularly critical issue, considering that the IVD contains a quiescent progenitor-like cell population that may be equipped to resist the hostile environment of degenerated IVD

tissue and to promote repair of the damaged tissue if properly stimulated (8,9). Therefore, it would be interesting to identify molecules as potential anti-IDD drugs based on natural products of plant origin capable of giving an adequate stimulus to the resident cells for reinitiating the anabolic machinery.

With this in mind and on the basis of our recent findings obtained in human bone cells (10), the present study aimed to investigate the potential effects of extracts from Violina pumpkin (*Cucurbita moschata*) leaves on the recovery of degenerated IVD cells. Until now, the properties of these leaves have not been well studied. Notably, these pumpkin leaves essentially represent a waste product of the plant, which are currently only appreciated in some countries of the world, such as Nigeria, Ghana, Tanzania, South and North Korea, and India, where traditional medicine has ascribed some healing properties to pumpkin leaves, including hepatoprotective, antidiabetic and anticancer properties (11-13), as well as antimicrobial, anti-inflammatory and antioxidant activity (14-16). Our recent study reported that extracts from the leaves of *C. moschata* exerted anabolic effects stimulating human osteoblast activity and inhibiting osteoclast differentiation (10). This dual effect has mainly been attributed to acetone-extractable substances, in particular fatty acids, such as 13-OH-9Z,11E,15E-octadecatrienoic acid (PU-13OH-FA), suggesting that bioactive chemicals from *C. moschata* leaves could be potentially useful for bone health. Among the acetone-extractable substances, two phenolic acids, ferulic acid and p-Coumaric acid, have also been identified in two different fractions. These phytochemicals, found in numerous vegetables and fruits, are believed to have no essential nutritional value but are effective in promoting beneficial effects on human health (17).

Previous evidence from the literature has indicated that ferulic acid may exert antioxidant effects on IVD cells (18,19). To the best of our knowledge, only one preliminary study has described the antioxidant and anti-senescence potential of p-Coumaric acid in IVD cells (20).

The present study aimed to explore whether the aforementioned substances have a beneficial effect on the biological repair of human damaged or degenerated IVD cells, or whether they exert a protective role. To test the hypothesis, the effects of acetone extracts of Violina pumpkin leaves were evaluated on human primary IVD cells from disc tissues with different levels of degeneration. The effect of treatment, measured in terms of discogenic phenotype and antioxidant responses, was also related to potential regulatory mechanisms that may be involved.

Materials and methods

Reagents and chemicals. All solvents were high-performance liquid chromatography (HPLC)-grade, and were purchased from Carlo ERBA Reagents srl, Honeywell Research Chemicals or Sigma-Aldrich; Merck KGaA. Thin layer chromatography (TLC) plates (Analtech Uniplates, silica gel GF, 20x20 cm, 500 μm) for preparative chromatography were purchased from Sigma-Aldrich; Merck KGaA. Gel column chromatography was performed on a packed column with silica gel (60, 70-230 mesh, Fluka®), which was also purchased from Sigma-Aldrich; Merck KGaA. MTT, 2,2'-azino-bis(3-ethylbenzothiazoline)-6-sulfonic acid (ABTS), 6-hydroxy-2,5,7,8-tetramethylchroman-2-carboxylic acid (Trolox), Folin-Ciocalteau reagent, potassium persulfate ($K_2S_2O_8$), sodium carbonate decahydrate ($Na_2CO_3 \cdot 10H_2O$), aluminium chloride ($AlCl_3$) hexahydrate, phenolic standards and flavonol standards were purchased from Sigma-Aldrich; Merck KGaA. Alexa Fluor 488 phalloidin (cat. no. A12379) was purchased from Thermo Fisher Scientific, Inc. The primary antibodies against SOX9 (cat. no. sc-20095), aggrecan (ACAN; cat. no. sc-33695), MMP13 (cat. no. sc-30073) Nrf2 (cat. no. sc-365949), sirtuin (SIRT)1 (cat. no. sc-74504), superoxide dismutase (SOD)2 (cat. no. sc-133134), OCT4 (cat. no. sc-5279), SOX2 (cat. no. sc-365823), FAS receptor (FasR; cat. no. sc-715) and Bcl-2 (cat. no. sc-7382) were purchased from Santa Cruz Biotechnology, Inc.; while FOXO3a (cat. no. ab70315) and collagen type II α1 chain (COL2a1; cat. no. ab3092) antibodies were purchased from Abcam; and anti-tricho-rhino-phalangeal syndrome type I protein, zinc finger protein (TRPS1; cat. no. 20003-1-AP) was purchased from ProteinTech Group, Inc. High-glucose Dulbecco's modified Eagle's medium (DMEM), Ham's F12 and 1X phosphate-buffered saline (PBS) were purchased from Euroclone S.p.A.

Preparation of pumpkin leaf extracts. Fresh Violina pumpkin (*C. moschata*) leaves were harvested in June 2021 at Alessandra Greco's farm (Agriturismo 'Alla Casella' Fondo Signa, Ferrara, Italy). The leaf extracts were prepared according to the procedures previously described by our research team (10). The leaves were washed, air dried for 2 weeks, cut into small pieces, homogenized to a fine powder and then stored in vacuum bags. Raw material (20 g) was extracted with 400 ml of each of the following solvents: N-hexane, acetone and methanol. Extractions were accomplished by three consecutive macerations (each extraction procedure was performed at room temperature for 48 h) to obtain hexane, acetone and methanol extracts as the final products (Fig. 1). Subsequently, the acetone extract was weighed and dissolved in neat DMSO to a final concentration of 30 mg/ml. The stock solution was serially diluted with growth medium for the different assays. The final concentration of DMSO in the cell culture medium in any experiment did not exceed 0.5%.

TLC. The acetone extract was resuspended in 2 ml dichloromethane-methanol (97.5:2.5), the same solvent mixture used as mobile phase for the elution, and applied as spots onto the dry stationary phase. After a complete run of 1 h, specific components were recovered by scraping the sorbent layer from the plate in the region of interest and eluting the separated material from the sorbent layer using a mixture of methanol and dichloromethane, followed by filtration and centrifugation (5,000 x g, room temperature, 5 min) to precipitate the silica gel. The supernatant was recovered and evaporated under vacuum. Three fractions of different polarity were recovered in an acceptable amount, and were identified as subfractions Fr2, Fr6 and Fr7. These fractions were further purified and characterized by nuclear magnetic resonance and by gas chromatography-mass spectrometry, as previously described (10), providing almost exclusively the hydroxy unsaturated fatty acid PU-13OH-FA (Fr2), 98.2% ferulic acid (Fr6) and 97.9% p-Coumaric acid (Fr7) (10).

Table I. TPC, TFC and antioxidant activities of Violina pumpkin leaf extract.

Extract	TPC, mg GAE/g dw	TFC, mg QE/g dw	TEAC, μmol TEAC/g dw
Acetone	21.8±0.98	9.65±0.79	3.9±0.5

dw, dry weight; GAE, gallic acid equivalent; QE, quercetin equivalent; TPC, total phenolic content; TFC, total flavonoid content; TEAC, Trolox Equivalent Antioxidant Capacity. Values are expressed as the mean ± standard deviation of three replicates.

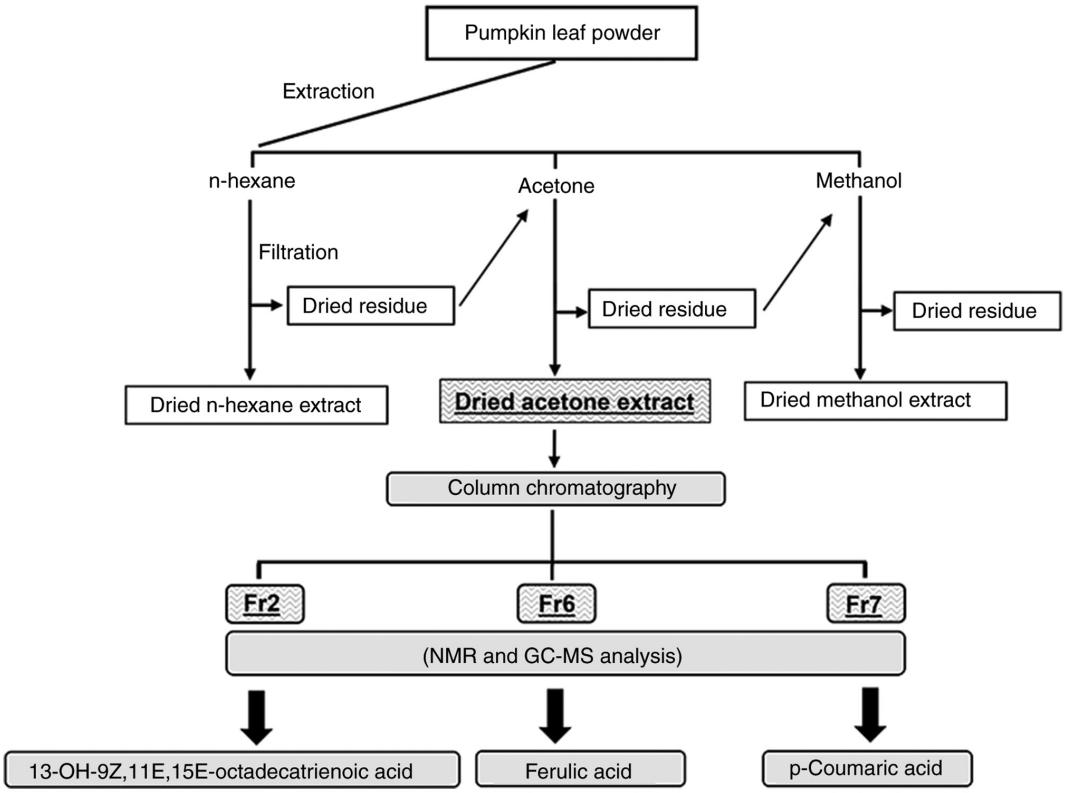

Figure 1. Schematic flow chart of the extraction and isolation process of compounds from Violina pumpkin (*Cucurbita moschata*) leaves (10). GC-MS, gas chromatography-mass spectrometry; NMR, nuclear magnetic resonance.

Determination of total phenolic and flavonoid contents in the acetone extract. Total polyphenol content (TPC) was determined using the Folin-Ciocalteu method (21). Briefly, 200 μl of the solution, obtained by redissolving the acetone extract from Violina pumpkin leaves in MeOH to reach a final concentration of 4,000 ppm, was diluted with distilled water (600 μl) and a 1:1 Folin-Ciocalteu reagent solution (200 μl) was added. After 5 min, a saturated solution of $Na_2CO_3 \cdot 10H_2O$ (1 ml) was added to the resulting mixture, finally diluting with distilled water to a total volume of 3 ml. This solution was kept in the dark at room temperature for 25 min, shaken using a vortex and subsequently, the absorbance was read at 765 nm. A gallic acid standard calibration curve (y=0.0035x-0.0061; r^2=0.9995) was generated by diluting the standard stock solution to obtain eight concentration levels in the range of 5-500 μg/l. The TPC was finally calculated as mg of gallic acid equivalents/g dry extract ± standard deviation (SD) (Table I).

Total flavonoid content (TFC) was assessed using the $AlCl_3$ method and quercetin was used as the reference. The calibration curve was drawn by preparing a set of eight standard solutions in the concentration range of 5-200 μg/ml (y=0.0149x + 0.0048; r^2=0.9990) by diluting the stock standard solution (5 mg/ml) using distilled water (1.0 ml). The diluted quercetin or the leaf extract solution (600 μl) were added at the same volume as a 2% w/v solution of $AlCl_3$. The resulting mixtures were allowed to react for 60 min at room temperature, and finally the absorbance was read against the blank at 420 nm. The TFC was expressed as mg of quercetin equivalent/g dry extract ± SD (Table I).

Determination of antioxidant capacity using ABTS radicals. The radical-scavenging activity of plant extracts was measured using the Trolox Equivalent Antioxidant Capacity (TEAC) assay with $ABTS^{\bullet+}$ cation radicals. The ABTS assay measures the relative ability of antioxidants to scavenge the $ABTS^{\bullet+}$ radical cation generated in the aqueous phase, as compared with a Trolox (water-soluble vitamin E analogue) standard. The general procedure reported by Re *et al* was followed (22). Briefly, ABTS was dissolved in distilled water to obtain a final concentration of 7 mM. Its radical cation ($ABTS^{\bullet+}$) was generated by the reaction

between ABTS stock aqueous solution (5 ml) and a strong oxidizing agent, such as $K_2S_2O_8$ (88 μl; 140 mM). The resulting mixture was kept in the dark at 26˚C for 12-16 h before use and then it was diluted with EtOH to reach an absorbance of 0.700 (±0.02) at 734 nm using a Varian Cary 50 UV-Vis spectrophotometer (Agilent Technologies, Inc.). Dry acetone extract from Violina pumpkin leaves (30 μl) was allowed to react with 2.97 ml of the resulting blue-green $ABTS^{\bullet+}$ radical solution in the dark at room temperature. The absorbance at the same wavelength was read after 2 min. The $ABTS^{\bullet+}$ scavenging capacity of the extracts was calculated as a percentage of inhibition=[(AB-AA)/AB] x100, where AA and AB represent the absorbance values of the $ABTS^{\bullet+}$ solution with and without the test samples, respectively. All tests were performed in triplicate. The results are expressed as TEAC values in μmol Trolox/g of dried material (Table I).

HPLC determination of phenolic acids and flavonoids. To identify the phenolic compounds in Violina pumpkin leaves, the acetone extracts previously obtained were resuspended in CH_3CN solution (containing 2 mg/ml tert-butylhydroquinone as an antioxidant) in a water bath at 85˚C for 1 h as described in the literature (23). After centrifugation (4,000 x g, room temperature, 5 min), the supernatant was filtered and analysed by HPLC. HPLC analyses were performed using an Agilent 1100 (Agilent Technologies, Inc.) series instrument equipped with an autosampler, a binary solvent pump and a diode-array detector. The separation was achieved employing a Supelco™ Kromasil® RP C18 HPLC column (Sigma-Aldrich; Merck KGaA) (4.6x150 mm; particle size, 5 μm). The mobile phase consisted of 0.4% formic acid in water (solvent A) and 0.4% formic acid (v/v) in acetonitrile solution (solvent B). The flow rate was adjusted to 0.8 ml/min, the column temperature was set at 25˚C and the injection volume was kept at 20 μl. The gradient was changed over time as follows: 0.0-20.0 min from 0 to 20% solvent B; 20.01-30.0 min 30% solvent B; 30.01-35.0 min from 30 to 50% solvent B; 35.01-45.0 min from 50 to 100% solvent B. Finally, the initial conditions of 0% solvent B were maintained for 10 min to re-equilibrate the HPLC column. The wavelength value for the identification and quantification was set at 320 and 326 nm for phenolic acids and flavonols, respectively, except for kaempferol, which was determined at a wavelength value of 370 nm. Each sample solution was filtered through a 0.22-μm Durapore® membrane (Sigma-Aldrich; Merck KGaA) before injection. The standard response curve for each phenolic acid was a linear regression fitted to values obtained at each of the eight concentrations (5,10, 50, 100, 200, 300, 400 and 500 μg/ml).

Cell isolation and cell culture. The present study was approved by the ethics committee of the University of Ferrara and University S. Anna Hospital (Ferrara, Italy) (protocol no. 160998; approved November 17, 2016). After written informed consent was obtained (in full accordance with The Declaration of Helsinki), a total of 24 herniated cervical IVD specimens were obtained from patients undergoing surgical discectomy, between March 2021 and June 2022. Patients with tumor infiltration, diabetes mellitus, spondylolisthesis, serious systemic disease, ankylosing spondylitis, HIV, HBV and HCV infections were excluded. The mean age of the donors was 53.2 years (range, 33-69 years) and there were nine women and 15 men (Table II). Nucleus pulposus tissue from each sample was macroscopically dissected from the annulus fibrosus and was subjected to enzymatic digestion using 1 mg/ml type IV collagenase (Sigma-Aldrich; Merck KGaA) for 5 h at 37˚C in DMEM/Ham's F12. Once the digestion was terminated, the cell suspension was filtered through a Falcon™ 70 μm Nylon Cell strainer (BD Biosciences). Subsequently, the cells were centrifuged at 300 x g for 10 min at room temperature, the supernatant was discarded, the cells were resuspended in basal medium [DMEM/F12 containing 10% foetal calf serum (FCS; Euroclone S.p.A), 100 mg/ml streptomycin, 100 U/ml penicillin and 1% Glutamine] and seeded in polystyrene culture plates (SARSTEDT AG & Co. KG) at a density of 10,000 cells/cm^2 and subcultured up to passage 3. Due to the small biopsy size and low proliferation rate of primary IVD cells in a monolayer, a single donor could not be used for all required experiments. Therefore, different donors were randomly assigned to the specific experiments (Table II).

Cell viability. To investigate cytotoxicity, IVD cells were seeded into 96-well plates at density of 3,000 cells/well and exposed to various concentrations (5, 50 and 250 μg/ml) of acetone extract and TLC subfractions (Fr2, Fr6 and Fr7). After 72 h at 37˚C, 0.5 mg/ml MTT was added to each well. After 3 h at 37˚C, the culture supernatant was removed from the wells and the formazan complex was dissolved in DMSO. The absorbance of each well was detected at 540 nm using a microplate reader (Sunrise™ Absorbance Reader; Tecan Group, Ltd.). Cell viability is expressed as a percentage of untreated control cells. To assess the protective effects of Violina pumpkin leaf extracts against H_2O_2-induced damage, IVD cells were pretreated with the DMSO (vehicle control), acetone extract or Fr7 (5 μg/ml) for 6 h and were then treated with different concentrations of H_2O_2 (0.25, 0.5 and 1 mM) and maintained for a further 16 h at 37˚C. Subsequently, the cells were analysed by MTT assay. The viability of DMSO-treated cells was set as 100%. Three replicates per treatment were assessed in three independent experiments.

For calcein AM/propidium iodide (PI) staining, cells were seeded in a 24-well plate at density of 10,000 cells/well, and were treated with DMSO (vehicle control), acetone extract (5 μg/ml) or TLC subfractions (Fr2, Fr6 and Fr7; 5 μg/ml) for 72 h. Before staining, the medium was removed from the wells, and 500 μl staining solution (Sigma-Aldrich; Merck KGaA) was added to each well. The samples were incubated in the dark at room temperature for 15 min, after which, the wells were rinsed with 1X PBS and immediately visualized under a fluorescence microscope (Nikon Eclipse 50i, Nikon Corporation). Dead cells were stained red, whereas viable cells appeared green.

Phalloidin staining. To evaluate the shape and structure of the cells, IVD cells were cultured in 24-well plates (10,000 cells/well) in the presence of 5 μg/ml acetone extract, Fr2, Fr6 or Fr7 for 72 h at 37˚C. Then, the cells were fixed with 4% paraformaldehyde for 2 min at 37˚C and permeabilized with 0.2% Triton X-100 in 1X PBS for 15 min. The cells were then stained with Alexa Fluor 488 phalloidin (1:500 dilution in 1X PBS) at room temperature in the dark for 30 min. Subsequently, the cells were washed with 1X

Table II. Clinical information of human IVD donors.

Donor	IVD level	Age, years	Sex	Symptoms	Duration of symptoms prior to surgery	Degeneration	Experiments performed
# 1	C4-C5	50	Male	Radiculopathy: pain and palsy	6 months	Mild	Viabilityassay/ Phalloidin staining
# 2	C6-C7	39	Male	Polytrauma	-	Severe	Immunocytochemistry
# 3	C7-T1	59	Male	Trauma, total cervical discectomy	-	Healthy	Scratch assay
# 4	C5-C6	67	Male	Radiculopathy: pain and palsy	10 months	Severe	Western blotting
# 5	C5-C6	38	Female	Radiculopathy; neck pain	2 months	Mild	Immunocytochemistry
# 6	C6-C7	65	Male	Radiculopathy: pain and palsy	2 months	Mild	Viability assay
# 7	C6-C7	45	Female	Radiculopathy: pain and palsy	12 months	Mild	Scratch assay
# 8	C5-C6	58	Female	Radiculopathy; neck pain	5 months	Mild	Western blotting
# 9	C4-C5	62	Male	Radiculopathy; neck pain	3 months	Mild	ROS assay
# 10	C5-C6	33	Female	Radiculopathy: pain and palsy	12 months	Mild	Immunocytochemistry
# 11	C4-C5	64	Male	Myelopathy	3 years	Severe	Viabilityassay/ Phalloidin staining
# 12	C6-C7	38	Female	Myelopathy	5 months	Severe	Viability assay
# 13	C5-C6	43	Male	Radiculopathy; neck pain	3 months	Mild	Immunocytochemistry
# 14	C6-C7	48	Female	Radiculopathy: pain and palsy	2 months	Severe	ROS assay
# 15	C6-C7	55	Male	Radiculopathy: pain and palsy	6 months	Mild	Viability assay/ Phalloidin staining
# 16	C4-C5	69	Female	Radiculopathy: pain and palsy	2 years	Severe	Immunocytochemistry
# 17	C5-C6	41	Female	Radiculopathy; neck pain	11 months	Severe	Western blotting
# 18	C5-C6	51	Female	Radiculopathy: pain and palsy	3 years	Severe	ROS assay
# 19	C4-C5	67	Male	Radiculopathy: pain and palsy	3 months	Severe	Scratch assay
# 20	C4-C5	68	Male	Radiculopathy: pain and palsy; neck pain	12 months	Severe	RT-qPCR
# 21	C4-C5	51	Male	Radiculopathy: pain and palsy	1 month	Mild	Viability assay
# 22	C3-C4	67	Male	Radiculopathy: pain and palsy	2 months	Severe	Immunocytochemistry
# 23	C5-C6	30	Male	Trauma	-	Mild	RT-qPCR
# 24	C4-C5	69	Male	Radiculopathy: pain and palsy	10 months	Severe	RT-qPCR

IVD, intervertebral disc; ROS, reactive oxygen species; RT-qPCR, reverse transcription-quantitative PCR.

PBS and the nuclei were counterstained with DAPI solution (Sigma-Aldrich; Merck KGaA). Fluorescent images were obtained using a fluorescence microscope (Nikon Eclipse 50i).

Scratch assay. The effects of acetone extract and TLC subfractions on cell migration were assessed *in vitro* using a scratch wound assay. Cells were seeded into 24-well plates and cultured until 80% confluence in 10% FCS-supplemented DMEM. The cells were then gently washed with 1X PBS and the medium was replaced with serum-free DMEM to prevent further cell proliferation. A scratch was made in the cell monolayer of each well using a sterile 200-μl pipette tip. Cellular debris was removed by washing with 1X PBS. Cells were then exposed to 5 μg/ml acetone extract, Fr2, Fr6 or Fr7 in serum-free medium. The scratches were examined by light microscopy and images were captured at 0 and 72 h after wound generation. Experiments were performed in triplicate. The healing area was semi-quantified using ImageJ 1.51 software (National Institutes of Health) and the results are expressed as a percentage of wound closure: (measurement at 0 h-measurement at 72 h)/measurement at 0 h x100.

Immunocytochemistry. Immunocytochemistry analysis was performed using the ImmPRESS kit (cat. no. MP-7500; Vector Laboratories, Inc.). Cells were plated at a density of 10,000 cells/cm^2 in 24-culture plates in the presence of 5 μg/ml acetone extract, Fr2, Fr6 or Fr7 for 72 h at 37˚C. Where required, cells were pretreated with acetone extract or Fr7 at 5 μg/ml for 6 h at 37˚C, before the addition of 500 μM H_2O_2 for 16 h at 37˚C. Next, cells were fixed in cold 100% methanol at room temperature for 10 min and permeabilized with 0.2% (v/v) Triton X-100 (Sigma-Aldrich; Merck KGaA) in 1X Tris-buffered saline (TBS) at room temperature for 10 min. Cells were treated with 3% H_2O_2 in 1X TBS at room temperature for 10 min and incubated in 2% normal horse serum (Vector Laboratories, Inc.) for 15 min at room temperature. After incubation in blocking serum, primary antibodies against SOX9 (1:500), TRPS1 (1:100), FOXO3a (1:1,000), ACAN (1:200), COL2a1 (1:200), MMP13 (1:200), FasR (1:500) and Bcl-2 (1:300), were added and incubated at 4˚C overnight. After rinsing in 1X TBS, the cells were incubated for 30 min at room temperature with ImmPRESS-HRP Universal Polymer reagent (horse anti-mouse/rabbit IgG) and then stained with substrate/chromogen mix (ImmPACT™ DAB) for 5 min at room temperature. After washing, the cells were mounted in glycerol/PBS (9:1) and observed under a Nikon Eclipse 50i optical microscope. Semi-quantitative image analysis of immunostained cells was performed using ImageJ software as previously reported (24).

Western blotting. For western blot analysis, after 72 h of exposure to acetone extract or Fr7 (5 μg/ml) at 37˚C, cells were washed with ice-cold 1X PBS and lysed with ice-cold RIPA buffer (50 mM Tris-HCl, pH 7.6; 1% NP-40; 150 mM NaCl; 1 mM NaF) containing a protease inhibitor cocktail (Sigma-Aldrich; Merck KGaA). Lysates were kept on ice for 30 min and centrifuged at 12,000 x g for 10 min at 4˚C. Protein concentration was quantified using the Bradford protein assay (Bio-Rad Laboratories, Inc.) with BSA (Sigma-Aldrich; Merck KGaA) as the standard. Total proteins (20 μg) were separated by SDS-PAGE on 10% gels and transferred to a PVDF membrane (MilliporeSigma) by electroblotting. Nonspecific binding was blocked with 5% (w/v) defatted milk powder in TBS-0.1% Tween-20 (TBST) for 1 h at room temperature, followed by incubation with primary antibodies against Nrf2 (1:1,000), SIRT1 (1:500), SOD2 (1:500), OCT4 (1:500) and SOX2 (1:500) in TBST overnight at 4˚C. After washing the PVDF membranes with TBST, blots were incubated with HRP-conjugated anti-rabbit (cat. no. P0448; Dako; Agilent Technologies, Inc.) or anti-mouse secondary antibodies (cat. no. P0447; Dako; Agilent Technologies, Inc.) (1:2,000) for 1 h at room temperature. Finally, protein expression was detected using Immobilon Western Chemiluminescent HRP Substrate (cat. no. WBKLS0500; MilliporeSigma). Anti-PI3K, p85 antibody (1:3,000; cat. no. 06-195; MilliporeSigma) was used as a loading control (25). PI3K was selected after various analyses that we have performed over the years, which suggested that its expression is very little influenced by biological factors (26,27). This is crucial when dealing with samples from different patients. Therefore, among the housekeeping proteins that are extensively used as loading controls, the abundance of PI3K has been shown to be relatively constant for the conditions and samples relevant to the experiments reported in the present study. Band intensities were semi-quantified by densitometric analysis using ImageJ software. All experiments were performed in triplicate.

Reactive oxygen species (ROS) detection. The level of intracellular ROS was determined using the 2,7-dichlorofluorescein diacetate (DCF-DA) assay (cat. no. 35845; Sigma-Aldrich; Merck KGaA). IVD cells were seeded in 96-well plates (1x10^4 cells/well) and cultured for 24 h. The cells were then pretreated with acetone extract or Fr7 at 5 μg/ml concentrations at 37˚C for 6 h, before the addition of 500 μM H_2O_2 at 37˚C for 16 h. The medium was then removed and the cells were incubated with DCF-DA (10 μM) in serum-free media at 37˚C for 30 min in the dark and the cells were washed with 1X PBS three times to diminish interference from excess DCF-DA. Fluorescence was determined using a microplate reader (SPECTRAFluorPlus; Tecan Group, Ltd.) at 485 nm (excitation) and 535 nm (emission), and was analysed using software Magellan V3.0 software (Tecan Group, Ltd.). The results are presented as the percentage of ROS production compared with in DMSO-treated control cells.

RNA isolation and reverse transcription-quantitative PCR (RT-qPCR). For miR-221 analysis, cells were pretreated with acetone extract or Fr7 (5 μg/ml) for 6 h, before the addition of 500 μM H_2O_2 for 16 h at 37˚C. Cells were then collected and total RNA, including microRNA (miRNA/miR), was extracted using the RNeasy® Plus Micro Kit (cat. no. 74034; Qiagen GmbH) according to the manufacturer's protocol. The amount and purity of the extracted RNA was evaluated by calculating 260/280 ratios using a NanoDrop ND1000 UV-VIS spectrophotometer (NanoDrop; Thermo Fisher Scientific, Inc.). cDNA was synthesized from total RNA according to manufacturer's protocol in a 20-μl reaction volume using the TaqMan miRNA RT kit (cat. no. 4366596; Thermo Fisher Scientific, Inc.). Quantification of miR-221 was performed using TaqMan MicroRNA Assays (hsa-miR-221-3p, cat. no. 000524; U6

small nuclear (sn)RNA, cat. no. 001973; Thermo Fisher Scientific, Inc.), using U6 snRNA for normalization. qPCR was performed with the TaqMan Universal PCR MasterMix II (cat. no. 4440040; Thermo Fisher Scientific, Inc.) using the CFX96TM PCR detection system (Bio-Rad Laboratories, Inc.) under the following amplification protocol: Initial denaturation at 95˚C for 10 min; followed by 40 cycles at 95˚C for 15 sec (denaturation step) and 60˚C for 1 min (annealing/extension step). Relative gene expression was calculated using the comparative $2^{-\Delta\Delta Cq}$ method (expressed as fold change) (28). All reactions were performed in triplicate and the experiments were repeated at least three times.

Statistical analysis. All experiments were performed at least three times. Data are expressed as the mean ± SD. Statistical analyses were performed using GraphPad Software version 8.0 (Dotmatics). Statistical differences were determined by one-way analysis of variance followed by Tukey's post hoc test for multiple comparisons. P<0.05 was considered to indicate a statistically significant difference.

Results

Effects of acetone leaf extract and TLC subfractions on degenerated IVD cells. Human IVD cells were isolated from the degenerated disc tissue of patients undergoing spinal surgery, characterized in terms of COL2a1, SOX9 and ACAN expression (data not shown) (29), and expanded up to passage three as previously described (29). After expansion, the cells become de-differentiated and lose their chondrogenic-like phenotype, becoming similar to cells undergoing the process of degeneration *in vivo*, as previously described (24). Based on previous evidence obtained in human osteoblasts (10), the cells were exposed to different concentrations (5, 50 and 250 μg/ml) of acetone extract from the leaves of *C. moschata* and three TLC subfractions (Fr2, Fr6 and Fr7), which were obtained as previously described (10). After 72 h, the MTT assay was performed. Only the highest concentrations were shown to be slightly (acetone extract and Fr7) or significantly (Fr2 and Fr6) cytotoxic (Fig. 2A). On the basis of these data, the subsequent experiments were carried out with treatments at a concentration of 5 μg/ml, which had no cytotoxic effect on the cells. Staining with calcein AM/PI confirmed that the cells were viable (Fig. 2B). Moreover, phalloidin staining showed no change in cytoskeletal organization or cellular morphology after treatment (Fig. 2C). Scratch assay was then performed and the wound-healing process was compared in cells exposed for 72 h to the different treatments. Notably, Fr7-treated cells showed a 69% wound closure, which was significantly higher than that of cells exposed to the other treatments (acetone extract, 24%; Fr2, 22%; Fr6, 28%; Fig. 3). The effect of Fr7 is interesting, considering that the migratory capacity of IVD cells is usually lost in the degenerated IVD microenvironment (30).

Effect of Fr7 on protein expression. Regarding the effect of treatment on expression, four groups of specific proteins were considered: i) Transcription factors with a recognized role in supporting the discogenic phenotype, namely SOX9 (a typical pro-chondrogenic transcription factor) (31), TRPS1 (an atypical

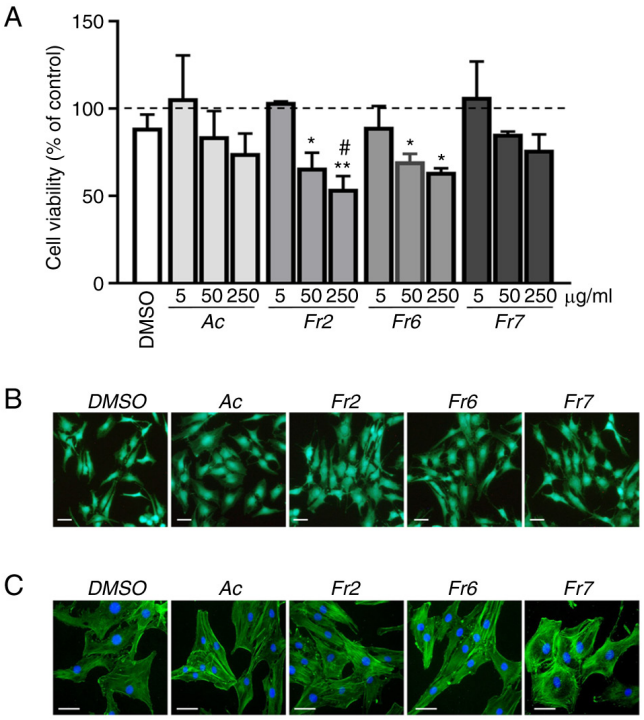

Figure 2. Effects of Violina pumpkin leaf extracts on cell viability. (A) IVD cells were treated with different concentrations (5, 50 and 250 μg/ml) of Ac or thin layer chromatography subfractions Fr2, Fr6 and Fr7 for 72 h. Cell viability was measured using the MTT assay. The viability of CTR cells was set at 100% (dotted line). Data are presented as the mean ± standard deviation (n=3). *P<0.05, **P<0.01 vs. CTR; $^{\#}$P<0.01 vs. DMSO. (B) IVD cells were treated with 5 μg/ml Ac, Fr2, Fr6 or Fr7 for 72 h. Cell viability was monitored by double staining with calcein AM/PI. Green fluorescence indicates the presence of calcein-labelled live cells, whereas PI-labelled dead cells are revealed by red fluorescence. Merged photomicrographs are shown. Scale bars, 20 μm. (C) IVD cells were treated with 5 μg/ml Ac, Fr2, Fr6 or Fr7 for 72 h and cytoskeletal organization was analysed by Alexa Fluor 488 phalloidin staining and fluorescence microscopy. Representative images of the cells are shown. Nuclei were counterstained with DAPI (blue). Scale bars, 10 μm. Ac, acetone extract; CTR, untreated control; IVD, intervertebral disc; PI, propidium iodide.

member of the GATA family that has recently been identified as a pro-discogenic factor) (29), and FOXO3a (an essential factor for the maturation and maintenance of IVD) (32); ii) factors involved in the maintenance of ECM homeostasis, namely ACAN and collagen type II (the most abundant structural components) (33), and MMP13 (a metalloprotease that serves key roles in ECM proteolysis in disc degeneration) (34); iii) crucial mediators of cellular defences against exogenous and endogenous stress, namely Nrf2 (a stress-responsive transcription factor) (35), SIRT1 (a deacetylase that stimulates antioxidant response) (36) and SOD2 (a mitochondrial antioxidant enzyme) (37); and iv) transcription factors related to resident stem/progenitor cells, namely OCT4 and SOX2 (38). Immunocytochemical analysis revealed that the expression levels of SOX9 and FOXO3a were significantly increased only by Fr7, whereas the expression of TRPS1 was significantly increased both by Fr6 and Fr7 (Fig. 4). ACAN was significantly increased both by Fr6 and Fr7, whereas Fr7 proved to be particularly effective in stimulating collagen type II expression (Fig. 5). Notably, the expression of MMP13 did not change in response to the different treatments (Fig. 5). These results indicated that Fr7 had a greater positive impact on

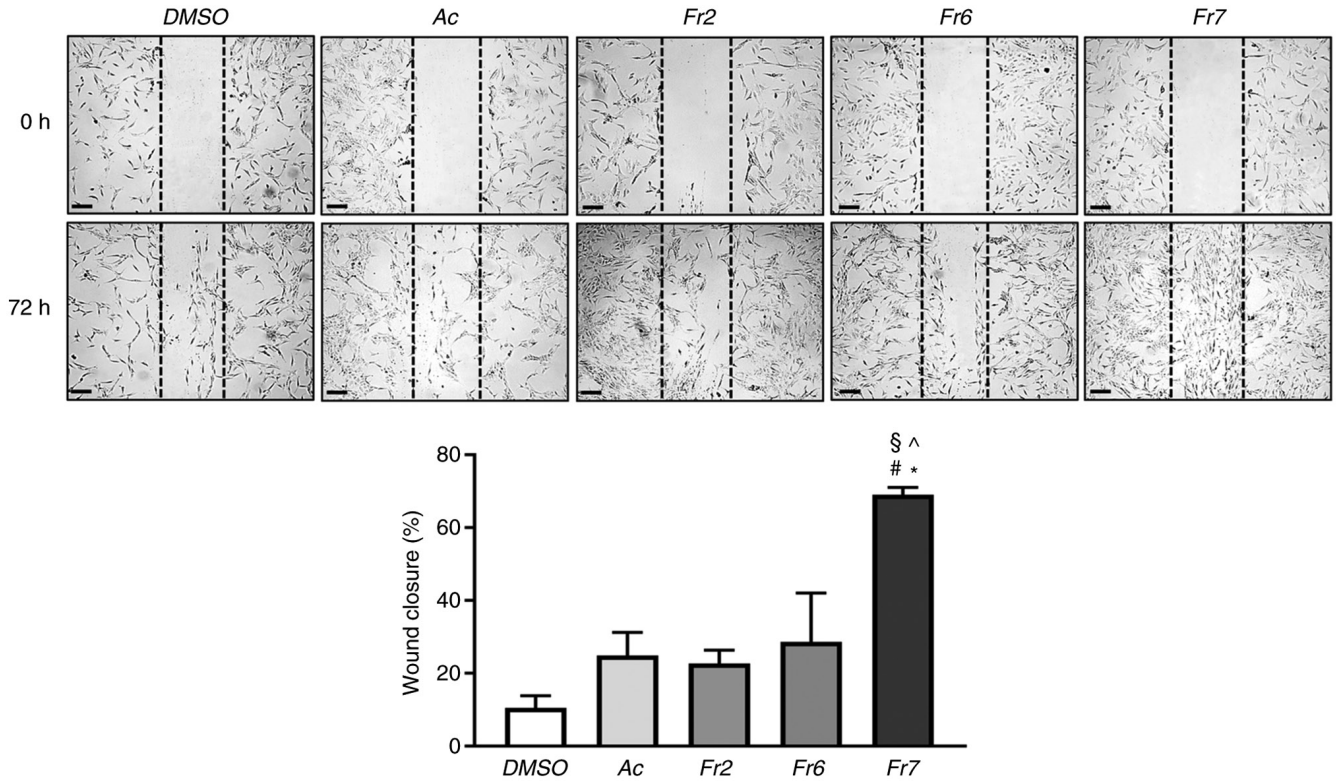

Figure 3. Effects of Violina pumpkin leaf extracts on the wound closure of IVD cells. IVD cells were treated with 5 μg/ml Ac, Fr2, Fr6 or Fr7 and subjected to wound scratch assay. Images were captured at 0 and 72 h. Quantitative evaluation and statistical analysis of wound closure percentage were measured using ImageJ software. Data are presented as the mean ± standard deviation (n=3). *P<0.01 vs. DMSO; $^{\#}$P<0.01 vs. Ac; §P<0.01 vs. Fr2; $^{\wedge}$P<0.01 vs. Fr6. Representative photomicrographs are shown. Scale bar, 50 μm. Ac, acetone extract; IVD, intervertebral disc.

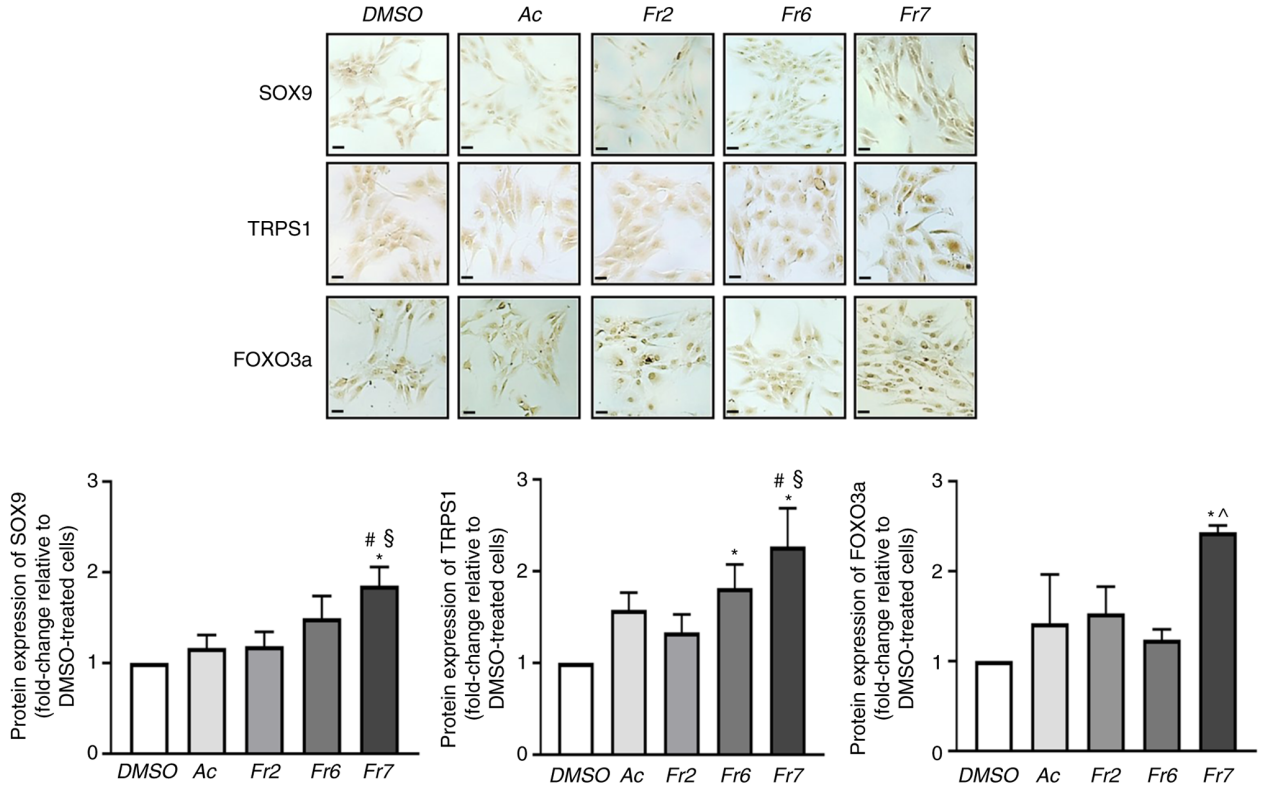

Figure 4. SOX9, TRPS1 and FOXO3a expression in intervertebral disc cells treated with Violina pumpkin leaf extracts. Protein expression levels were evaluated by immunocytochemistry following treatment with 5 μg/ml Ac, Fr2, Fr6 or Fr7 for 72 h. Representative optical photomicrographs of immunostaining are shown. Scale bars, 20 μm. Protein levels were semi-quantified by densitometric analysis of immunocytochemical staining using ImageJ software and are expressed as fold change relative to DMSO-treated cells. Data are presented as the mean ± SD (n=3). *P<0.05 vs. DMSO; $^{\#}$P<0.05 vs. Ac; §P<0.01 vs. Fr2; $^{\wedge}$P<0.05 vs. Fr6. Ac, acetone extract; TRPS1, tricho-rhino-phalangeal syndrome type I protein, zinc finger protein.

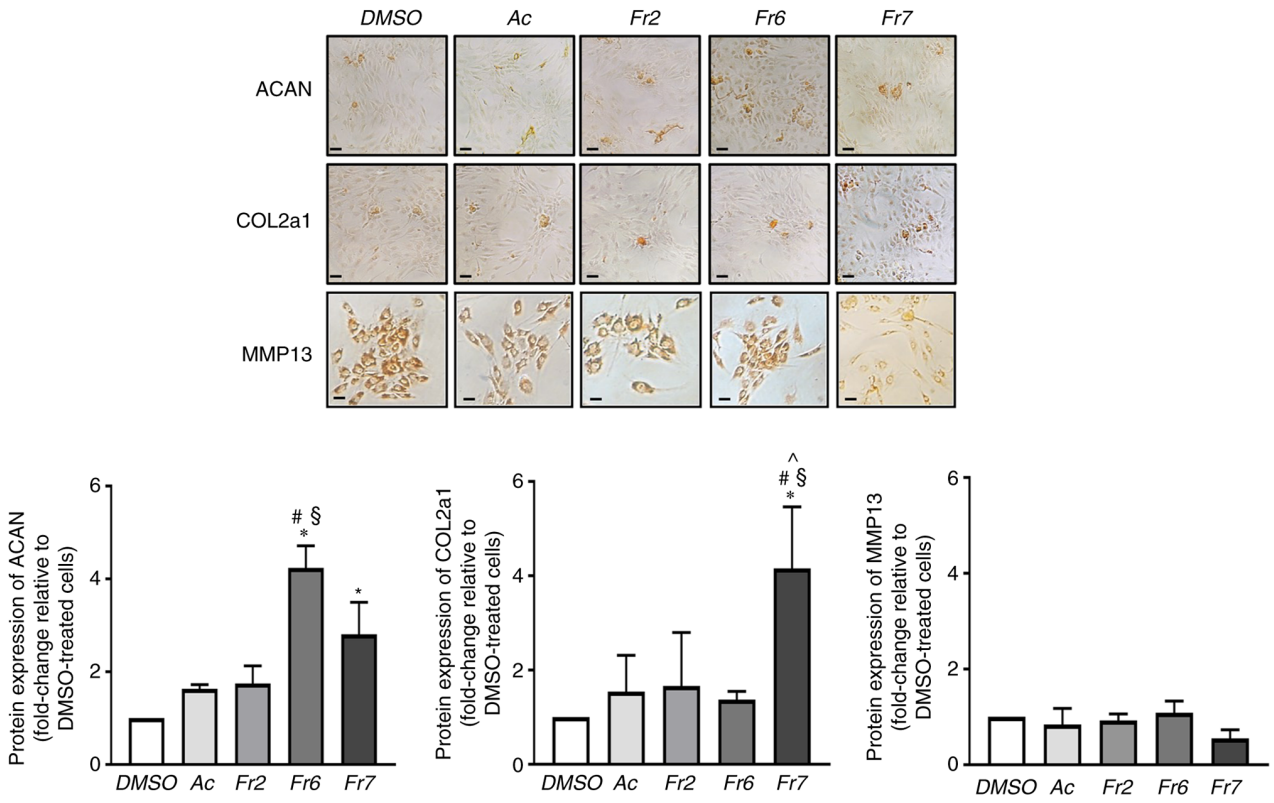

Figure 5. ACAN, COL2a1 and MMP13 expression in intervertebral disc cells treated with Violina pumpkin leaf extracts. Protein expression levels were evaluated by immunocytochemistry following treatment with 5 μg/ml Ac, Fr2, Fr6 or Fr7 for 72 h. Representative optical photomicrographs of immunostaining are shown. Scale bars, 20 μm. Protein levels were semi-quantified by densitometric analysis of immunocytochemical staining using ImageJ software and are expressed as fold change relative to DMSO-treated cells. Data are presented as the mean ± SD (n=3). *P<0.05 vs. DMSO; #P<0.05 vs. Ac; §P<0.05 vs. Fr2; ^P<0.05 vs. Fr6. Ac, acetone extract; ACAN, aggrecan; COL2a1, collagen type α1 chain.

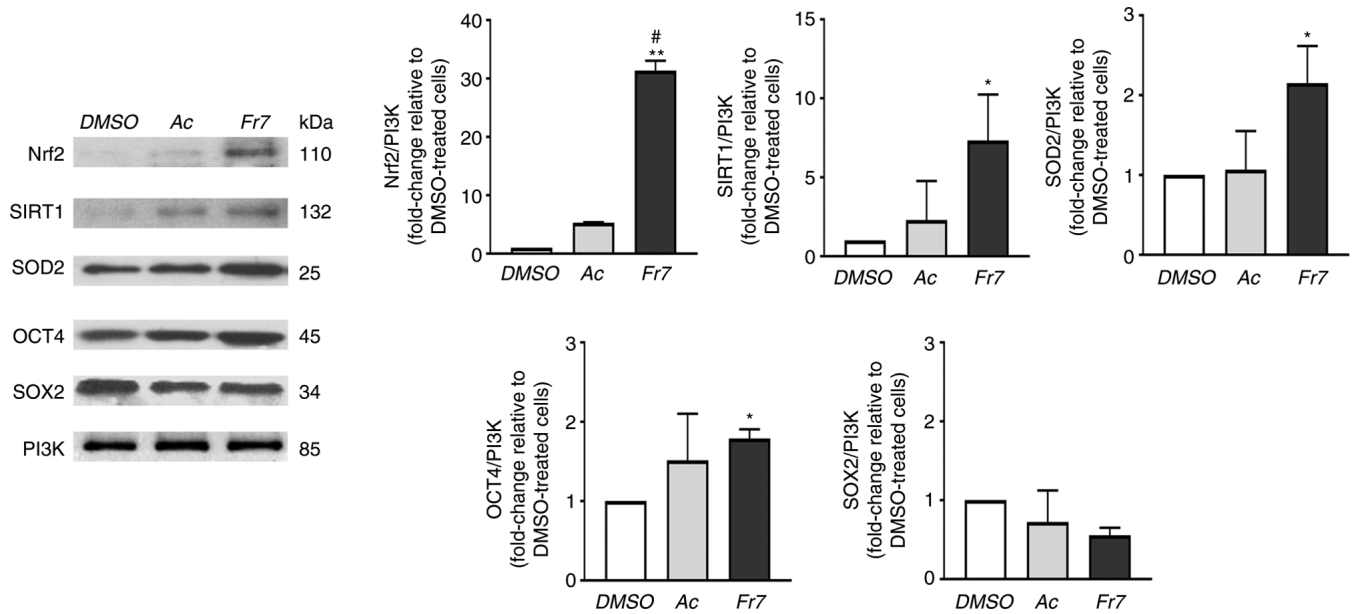

Figure 6. Nrf2, SIRT1, SOD2, OCT4 and SOX2 expression in intervertebral disc cells treated with Violina pumpkin leaf extracts. Protein expression levels were evaluated by western blotting after treatment with 5 μg/ml Ac or Fr7 for 72 h. Representative western blots are presented. Relative protein expression levels were calculated by densitometry and the results are presented as fold change relative to DMSO-treated cells. Data are presented as the mean ± SD (n=3). PI3K was used as a loading control. *P<0.05, **P<0.01 vs. DMSO; #P<0.01 vs. Ac. Ac, acetone extract; Nrf2, nuclear factor erythroid 2-related factor 2; SIRT1, sirtuin 1; SOD2, superoxide dismutase 2.

degenerated IVD cells than the other fractions. The subsequent experiments compared Fr7 with the acetone extract. As shown in Fig. 6, the expression levels of all three proteins related to antioxidants and redox signalling (Nrf2, SIRT1 and SOD2)

were significantly upregulated by Fr7, and Fr7 also positively affected OCT4 expression. Conversely, SOX2 expression was not significantly affected by treatments (Fig. 6). These findings suggested that Fr7 may affect stemness maintenance. In future, it will be interesting to improve understanding regarding this and to identify the specific action of molecules contained in Fr7 that may affect IVD endogenous stem cell niche activity.

Collectively, these data are in agreement with the antioxidant capacity assignable to the phenolic acids and flavonols that were identified and quantified by HPLC analysis in the acetone extract (Table III). Notably, the subfraction with the greatest biological effect, Fr7, consisted almost entirely (97.9%) of p-Coumaric acid as previously reported (10), and contains traces of gallic acid and protocatechuic acid (data not shown). It is well accepted that the low number of IVD cells that can be obtained by a disc biopsy limits the number of feasible experiments. However, in the future it will be interesting to evaluate the effects of pure p-Coumaric acid and to investigate the possible synergistic action of the minor components present only in traces.

Fr7 mitigates H_2O_2-triggered cell damage. The results presented so far refer to the intrinsic capacity of the cells to respond to molecules contained in the leaf extract. To further validate the properties of the extract, and, in particular, to propose a potential mechanism of action of the major component of Fr7, p-Coumaric acid, the ability of the IVD cells to counteract the damage induced by H_2O_2 when exposed to Fr7 was assessed.

The cells were subjected to different dosages of H_2O_2 (0.25, 0.5 and 1 mM) and cell viability was subsequently detected using the MTT assay. The cells showed a significant decrease in viability in response to 0.5 mM H_2O_2 compared with in the DMSO-treated group (Fig. 7A); therefore, subsequent analyses were performed using this concentration. Notably, exposure to Fr7 promoted a modest but significant resistance to stress induced by H_2O_2. As expected, H_2O_2 induced the expression of a pro-apoptotic factor, FasR and decreased the expression of an anti-apoptotic protein, Bcl-2 (39,40). Notably, this effect was counteracted by the acetone extract and even more so by Fr7 treatment (Fig. 7B). In addition, Fr7 relieved H_2O_2-triggered ROS production by the cells (Fig. 7C).

Subsequently, the present study evaluated the ability of Fr7 to interfere with possible molecular mediators of H_2O_2 action, such as specific miRNAs. It is well known that H_2O_2-triggered cell damage is also accompanied by changes in the levels of miRNAs participating in multiple cell responses (41). In the present study, the effectiveness of exposure to Fr7 was evaluated by monitoring the modulation of a powerful regulator of numerous cell functions, miR-221. Among the several roles played by this miRNA, its involvement as a negative regulator of chondrogenesis and as a mediator of inflammatory pathways is relevant (42,43). The choice to evaluate this miRNA comes from our previous evidence showing that miR-221 expression was increased with the degree of IVD degeneration, and that, consistently, its silencing was effective in changing the degenerated phenotype of IVD cells and restoring the chondrogenic-like phenotype (29). As shown in Fig. 7D, exposure to H_2O_2 significantly increased the expression levels of miR-221, whereas the expression levels of miR-221 were significantly decreased in cells that were pretreated with acetone extract and even more so with Fr7.

Table III. Content of phenolic acids and flavonols in Violina pumpkin leaf acetone extract.

A, Phenolic acids	
Compound	Amount, μg/g dw
Gallic acid	91.0±1.1
Protocatechuic acid	5.9±0.69
Cinnamic acid	8.12±0.21
Gentisic acid	301±1.7
p-Hydroxybenzoic acid	5.1±0.87
Caffeic acid	287.8±0.001
p-Coumaric acid	398.1±1.2
Ferulic acid	176.3±0.82
B, Flavonols	
Compound	Amount, μg/g dw
Rutin	98.3±0.91
Kaempferol	85.23±0.83
Astragalin	83.4±0.70
Myricetin	81.23±0.65
Quercetin	76±0.29

dw, dry weight. Values are expressed as the mean ± standard deviation of three replicates.

Discussion

The present study adds a new plant extract (Violina pumpkin leaf extract) and a molecule contained in it (p-Coumaric acid) to a list of natural compounds hitherto proposed as potential drugs for the treatment of IVD degeneration (5). The research in this field is rapidly increasing. The properties of a number of these compounds, including inhibition of oxidative stress, inflammation, apoptosis and ECM degradation, along with their regulatory effects on molecular pathways related to the pathogenesis of IDD have been highlighted in recent reviews (5,44). However, we are still far from developing therapeutic protocols based on natural plant-derived compounds for the treatment of this disease. This is mainly due to the lack of knowledge on the mechanisms of action of the variety of natural products isolated from plants, the variability of the experimental models employed, as well as the difficulty of recreating an *in vitro* microenvironment that closely mimics the human one.

With this last issue in mind, the present study used primary IVD cells obtained from human biopsies; to the best of our knowledge, the present study demonstrated for the first time the intrinsic ability of these cells to respond to molecules contained in the acetone extract from the leaves of *C. moschata*. In particular, the cells were responsive to Fr7,

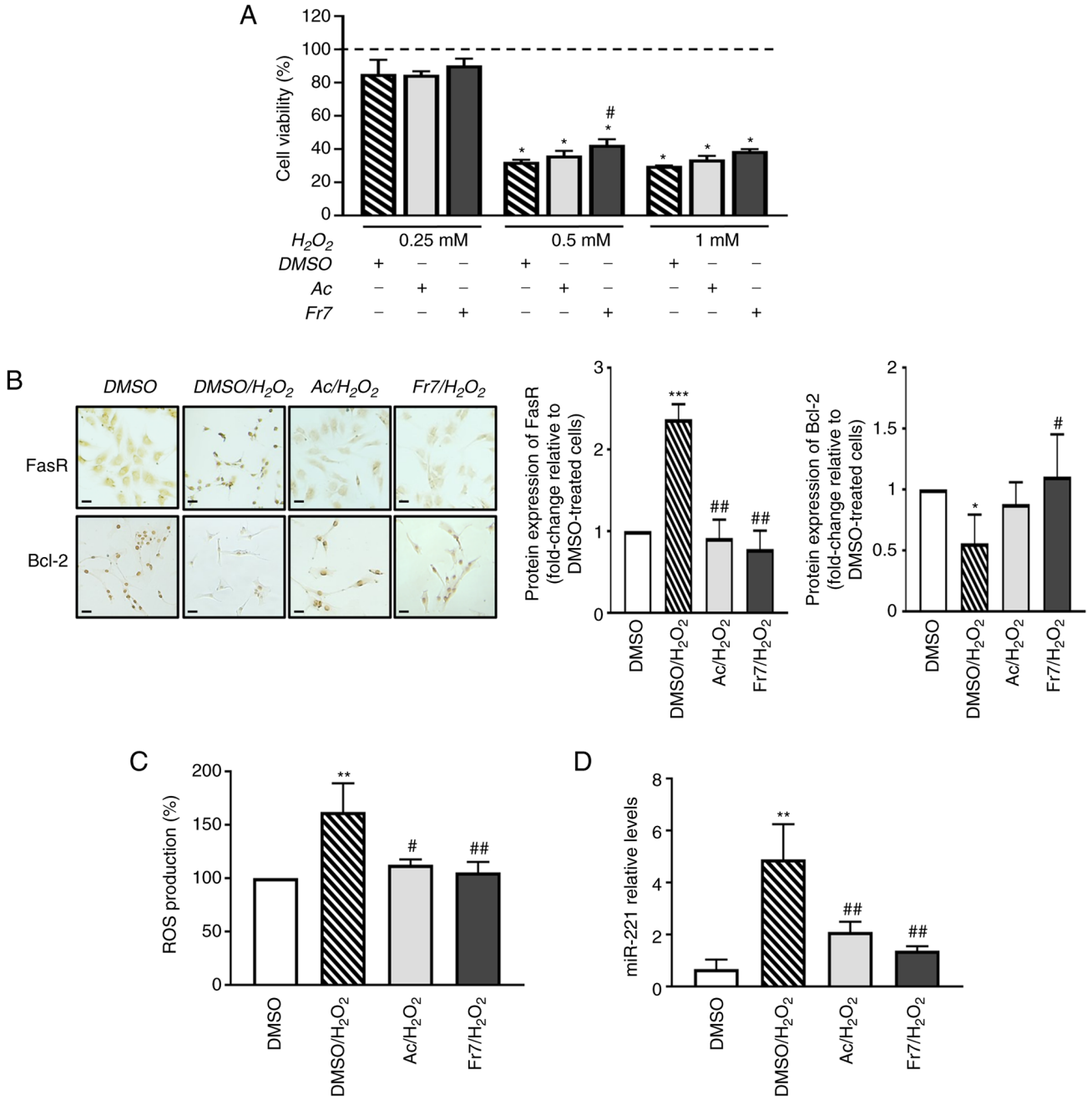

Figure 7. Effects of Ac and Fr7 of Violina pumpkin leaves on damage induced by H_2O_2. (A) IVD cells were pretreated with 5 μg/ml Ac or Fr7 for 6 h and then cultured with different concentrations of H_2O_2 for 16 h. Cell viability was measured using the MTT assay. The viability of DMSO-treated cells was set as 100% (dotted line). Data are presented as the mean ± SD (n=3). *P<0.01 vs. DMSO; $^{\#}$P<0.05 vs. DMSO/H_2O_2 (0.5 mM). IVD cells were pretreated with 5 μg/ml Ac or Fr7 for 6 h and then cultured with 0.5 mM H_2O_2 for 16 h. (B) Protein expression levels of pro-apoptotic FasR and anti-apoptotic Bcl-2 were evaluated by immunocytochemistry. Representative optical photomicrographs of immunostaining are shown. Scale bars, 20 μm. Protein levels were semi-quantified by densitometric analysis of immunocytochemical staining using ImageJ software and are expressed as fold change relative to DMSO-treated cells. Data are presented as the mean ± SD (n=3). (C) Intracellular ROS production was evaluated. ROS levels are presented as a percentage relative to DMSO-treated cells. Data are presented as the mean ± SD (n=3). (D) Expression levels of miR-221 relative to U6 small nuclear RNA expression were determined by reverse transcription-quantitative PCR. Expression levels are presented as fold change relative to DMSO-treated cells and the data are expressed as the mean ± SD (n=3). *P<0.05, **P<0.01, ***P<0.001 vs. DMSO; $^{\#}$P<0.05, $^{\#\#}$P<0.01 vs. DMSO/H_2O_2. Ac, acetone extract; FasR, FAS receptor; H_2O_2, hydrogen peroxide; IVD, intervertebral disc; miR-221, microRNA-221; ROS, reactive oxygen species.

which consisted almost entirely of p-Coumaric acid (97.9%), a molecule known for its scavenging and antioxidative properties in the reduction of oxidative stress and inflammatory reactions, diabetes mitigation, neuroprotective action, antineoplastic and antimicrobial activity (45,46). Treatment with Fr7 induced an increase in discogenic transcription factors (SOX9, TRPS1), ECM components (ACAN and collagen type II), and regulators of cellular homeostasis and stress response (FOXO3a, Nrf2, SOD2 and SIRT1). This was accompanied by a significant effect on another important aspect regarding stem/progenitor cells, which have recently been found in the IVD cell population (8). Notably, exposure to Fr7 revealed a cellular response attributable to stem cell activity, i.e. an increase in cellular migratory ability and

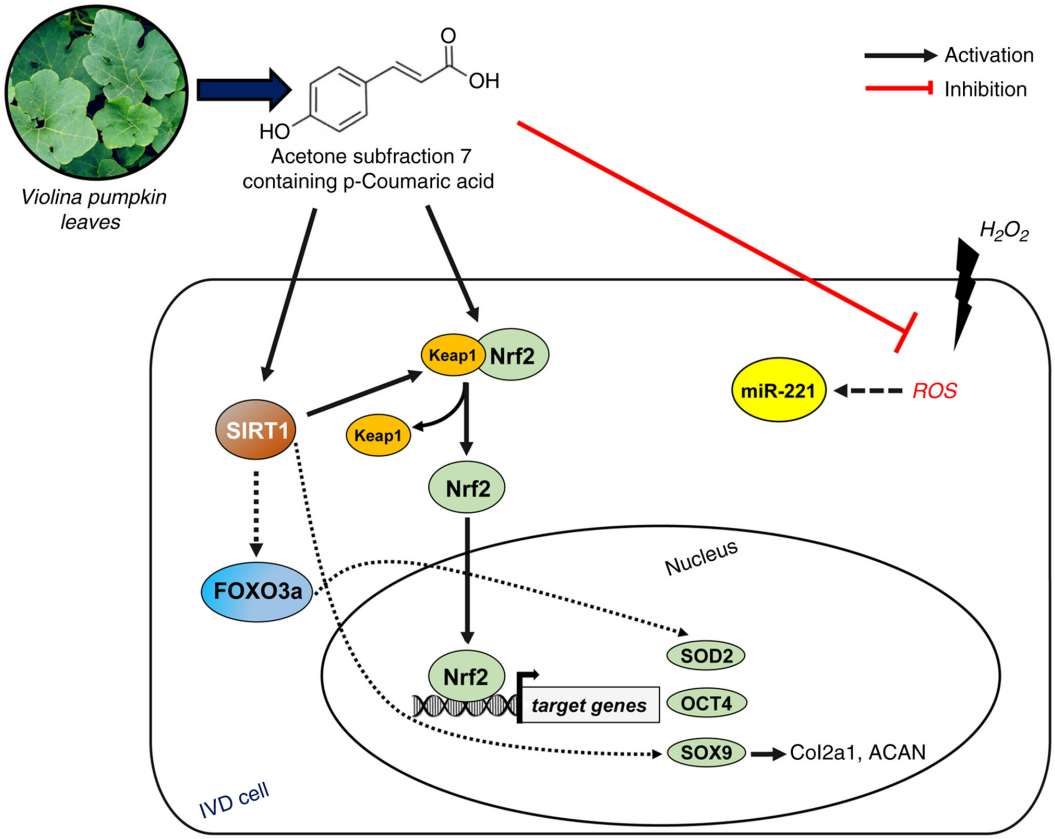

Figure 8. Schematic diagram showing the potential effects of subfraction 7 of Violina pumpkin leaf extract on the recovery of degenerated IVD cells. ACAN, aggrecan; H_2O_2, hydrogen peroxide; IVD, intervertebral disc; miR-221, microRNA-221; ROS, reactive oxygen species; SIRT1, sirtuin 1; SOD2, superoxide dismutase 2.

expression of OCT4, which is essential for the pluripotency and self-renewal capacity of stem cells. This strengthens the hypothesis that adequate stimuli can support resident cells to repopulate the degenerated IVD and reinitiate the anabolic machinery. We are confident that stem/progenitor cells are among the cells that reside in the IVD microenvironment, which is constitutively characterized by poor regenerative/reparative capacity (38).

There is an objective difficulty in identifying ideal drug candidates that meet the principles of regenerative medicine, which aims to restore IVD function via small-molecule drugs (47). Due to anatomical and functional complexity, the interactions that IVD cells establish with different components of the microenvironment and the ability they have to react to injuries are not yet well understood. Notably, in this scenario, plant extracts can help, as several studies have shown that certain compounds from plants act as bioactive mediators in regulating the rate of cell division, differentiation, tissue regeneration and immunomodulation through complex signalling pathways, such as BMP2, TNF-α, NF-κB, mTOR, JAK2/STAT3, Runx2 and Wnt (5,48). Therefore, combining the evidence obtained in the present study alongside previous literature, it is reasonable to hypothesize that Fr7-treated cells responded with different regulatory signals aimed at restoring IVD homeostasis, including those proposed in the schematic diagram shown in Fig. 8. The diagram shows three different directions through which p-Coumaric acid may exert its effect: i) reduction in ROS generation; ii) activation of Nrf2 by destabilizing the association with its negative regulator Keap1; iii) acting as a SIRT-activating compound, increasing the enzymatic activity of SIRT1. SIRT1 can deacetylate and activate the longevity transcription factor FOXO3a, thus leading to the modulation of several target genes (49). Free Nrf2 enters the nucleus and binds antioxidant response elements to initiate the transcriptional expression of SOD2 (50), OCT4 (51) and SOX9 (52). In turn, SOX9, recently shown to also be a target of SIRT1 (53), can trigger the transcription of collagen type II, ACAN and TRPS1 (54,55). We are currently unable to determine the temporal dynamics driven by transcriptional regulation. Most likely, the activation of a cell damage sensor, such as Nrf2, plays a key role and promptly ensures both repair and functional restoration phenomena (56,57).

In the present study, the effects of exposure to H_2O_2 highlighted another important area that will certainly require further investigation, namely the importance of maintaining low levels of miR-221, a pro-inflammatory and anti-chondrogenic miRNA (42), in order to restore the discogenic phenotype (29). Notably, Fr7 was able to counteract the large H_2O_2-mediated increase in miR-221, demonstrating that the ability of p-Coumaric acid to promote differentiation may also be explained by hindering anti-chondrogenic molecules. It has been reported that changes in cellular concentrations of specific miRNAs are associated with the levels of ROS producers and ROS scavengers through specific circuits (41). Therefore, it is possible that p-Coumaric acid may participate in adjusting the

IVD redox microenvironment to achieve optimal ROS levels for specific cellular processes. It will be interesting to evaluate which of the potential signalling pathways are preferential targets of miR-221 during the IVD degeneration process.

Taken together, the data obtained suggested that the p-Coumaric acid contained in Fr7 exerted not only anti-inflammatory and anti-catabolic properties, but also anabolic properties and pro-differentiating effects on the primary culture of degenerated human IVD cells. This is a particularly critical issue. Identifying compounds as anti-IVD degeneration drugs based on natural products of plant origin that are capable of providing an adequate tissue repair/regeneration stimulus opens the way to alternative therapies. However, small molecule-based therapy can only be developed if knowledge about the mechanisms that control different pathways of IVD homeostasis increases (47). It is worth noting that small molecule-based therapy also involves the possible incorporation of specific compounds, such as p-Coumaric acid, into biomaterials to produce so-called 'herbal scaffolds' for IVD tissue engineering. The development of biomaterials combined with bioactive plant extracts aims to increase the regenerative potential of the scaffold and to create a controlled release system that is crucial to ensure the presence of herbal extracts for a prolonged period in the site of damage, as recently proposed for bone fracture healing (58).

In conclusion, the present study demonstrated that Violina pumpkin leaves contain acetone-extractable substances, including p-Coumaric acid, which are effective in restoring the metabolic activity of degenerated human IVD cells, counteracting the inflammation and loss of the chondrogenic phenotype, favouring antioxidant defence and the activity of stem cells. Considering that combination effects (including both synergy and antagonism) have been described in a number of natural product extracts (59,60), and that p-Coumaric acid represents 97.9% of Fr7, it cannot be excluded that gallic acid and protocatechuic acid, which were found only in traces, may also serve a biological role; this will be the subject of future investigations.

The evidence reported in the present study offers interesting insights into different molecular mechanisms responsible for IVD homeostasis and may aid in the development of novel molecule-based therapeutics against IVD degeneration. Moreover, although further studies on the properties of pumpkin leaves are needed, it is worth encouraging in general the enhanced use of this part of the plant in Western countries, which still consider them to be mainly a waste product.

Acknowledgements

The authors would like to thank Professor Pasquale De Bonis (Department of Neurosurgery, University S. Anna Hospital of Ferrara) for providing human IVD biopsies.

Funding

This study was supported by Roberta Piva and Letizia Penolazzi Funds from the University of Ferrara (Fondo di Ateneo per la Ricerca Scientifica 2021), and by Assunta Pandolfi with the PON-MISE Sustainable Growth Funding-DD 27/09/2018, Prog.n. F/180021/01-04/X43.

Availability of data and materials

The datasets used and/or analysed during the current study are available from the corresponding author on reasonable request.

Authors' contributions

EL and LP performed the experiments, data curation and drafted the manuscript. MPN and SF helped to perform the experiments and data curation. FE contributed to data analysis and interpretation, and reviewed and supervised the study. AP designed the study, supervised data analysis and raised funding. RP designed and supervised the study, raised funding, analysed the data and wrote the manuscript. EL, FE and RP confirm the authenticity of all the raw data. All authors have read and approved the final manuscript.

Ethics approval and consent to participate

The present study was approved by the ethics committee of the University of Ferrara and S. Anna Hospital (protocol no. 160998; approved November 17, 2016). Written informed consent was obtained prior to the collection of herniated cervical IVD specimens from 24 donors undergoing surgical discectomy.

Patient consent for publication

Not applicable.

Competing interests

The authors declared that they have no competing interests.

References

1. Knezevic NN, Candido KD, Vlaeyen JWS, Van Zundert J and Cohen SP: Low back pain. Lancet 398: 78-92, 2021.
2. Urits I, Burshtein A, Sharma M, Testa L, Gold PA, Orhurhu V, Viswanath O, Jones MR, Sidransky MA, Spektor B and Kaye AD: Low back pain, a comprehensive review: Pathophysiology, diagnosis, and treatment. Curr Pain Headache Rep 23: 23, 2019.
3. Lyu FJ, Cui H, Pan H, Mc Cheung K, Cao X, Iatridis JC and Zheng Z: Painful intervertebral disc degeneration and inflammation: From laboratory evidence to clinical interventions. Bone Res 9: 7, 2021.
4. Lawson LY and Harfe BD: Developmental mechanisms of intervertebral disc and vertebral column formation. Wiley Interdiscip Rev Dev Biol 6: e283, 2017.
5. Chen HW, Zhang GZ, Liu MQ, Zhang LJ, Kang JH, Wang ZH, Liu WZ, Lin AX and Kang XW: Natural products of pharmacology and mechanisms in nucleus pulposus cells and intervertebral disc degeneration. Evid Based Complement Alternat Med 2021: 9963677, 2021.
6. Song D, Ge J, Wang Y, Yan Q, Wu C, Yu H, Yang M, Yang H and Zou J: Tea polyphenol attenuates oxidative stress-induced degeneration of intervertebral discs by regulating the Keap1/Nrf2/ARE pathway. Oxid Med Cell Longev 2021: 6684147, 2021.
7. Wang D, Cai X, Xu F, Kang H, Li Y and Feng R: Ganoderic acid A alleviates the degeneration of intervertebral disc via suppressing the activation of TLR4/NLRP3 signaling pathway. Bioengineered 13: 11684-11693, 2022.
8. Lyu FJ, Cheung KM, Zheng Z, Wang H, Sakai D and Leung VY: IVD progenitor cells: A new horizon for understanding disc homeostasis and repair. Nat Rev Rheumatol 15: 102-112, 2019.
9. Wang J, Huang Y, Huang L, Shi K, Wang J, Zhu C, Li L, Zhang L, Feng G, Liu L and Song Y: Novel biomarkers of intervertebral disc cells and evidence of stem cells in the intervertebral disc. Osteoarthritis Cartilage 29: 389-401, 2021.

10. Lambertini E, Penolazzi L, Pellielo G, Pipino C, Pandolfi A, Fiorito S, Epifano F, Genovese S and Piva R: Pro-osteogenic properties of Violina pumpkin (*Cucurbita moschata*) leaf extracts: Data from in vitro human primary cell cultures. Nutrients 13: 2633, 2021.
11. Adaramoye OA, Achem J, Akintayo OO and Fafunso MA: Hypolipidemic effect of *Telfairia occidentalis* (fluted pumpkin) in rats fed a cholesterol-rich diet. J Med Food 10: 330-336, 2007.
12. Eseyin OA, Igboasoiyi AC, Mbagwu H, Umoh E and Ekpe JF: Studies on the effects of an alcohol extract of the leaves of Telfairia occidentalis on alloxan induced diabetic rats. Global J Pure Appl Sci 11: 77-79, 2005.
13. Igbeneghu OA and Abdu AB: Multiple antibiotic-resistant bacteria on fluted pumpkin leaves, a herb of therapeutic value. J Health Popul Nutr 32: 176-182, 2014.
14. Oboh G, Nwanna EE and Elusiyan CA: Antioxidant and antimicrobial properties of *Telfairia occidentalis* (Fluted pumpkin) leaf extracts. J Pharmacol Toxicol 1: 167-175, 2006.
15. P N O: Effect of aqueous extract of Telfairia occidentalis leaf on the performance and haematological indices of starter broilers. ISRN Vet Sci 2012: 726515, 2012.
16. Aderibigbe AO, Lawal BA and Oluwagbemi JO: The antihyperglycamic effect of *Telfaria occidentalis* in mice. Afr J Med Med Sci 28: 171-175, 1999.
17. van Breda SGJ and de Kok TMCM: Smart combinations of bioactive compounds in fruits and vegetables may guide new strategies for personalized prevention of chronic diseases. Mol Nutr Food Res 62: 1700597, 2018.
18. Cheng YH, Yang SH and Lin FH: Thermosensitive chitosan-gelatin-glycerol phosphate hydrogel as a controlled release system of ferulic acid for nucleus pulposus regeneration. Biomaterials 32: 6953-6961, 2011.
19. Cheng YH, Yang SH, Yang KC, Chen MP and Lin FH: The effects of ferulic acid on nucleus pulposus cells under hydrogen peroxide-induced oxidative stress. Process Biochem 46: 1670-1677, 2011.
20. Sheng K, Li Y, Wang Z, Hang K and Ye Z: p-Coumaric acid suppresses reactive oxygen species-induced senescence in nucleus pulposus cells. Exp Ther Med 23: 183, 2022.
21. Chandra S, Khan S, Avula B, Lata H, Yang MH, ElSohly MA and Khan IA: Assessment of total phenolic and flavonoid content, antioxidant properties, and yield of aeroponically and conventionally grown leafy vegetables and fruit crops: A comparative study. Evid Based Complement Alternat Med 2014: 253875, 2014.
22. Re R, Pellegrini N, Proteggente A, Pannala A, Yang M and Rice-Evans C: Antioxidant activity applying an improved ABTS radical cation decolorization assay. Free Radic Biol Med 26: 1231-1237, 1999.
23. Xu W, Liu L, Hu B, Sun Y, Ye H, Ma D and Zeng X: TPC in the leaves of 116 sweet potato (*Ipomoea batatas* L.) varieties and Pushu 53 leaf extracts. J Food Compos Anal 23: 599-604, 2010.
24. Penolazzi L, Lambertini E, Scussel Bergamin L, Gandini C, Musio A, De Bonis P, Cavallo M and Piva R: Reciprocal regulation of TRPS1 and miR-221 in intervertebral disc cells. Cells 8: 1170, 2019.
25. Nunes de Miranda SM, Wilhelm T, Huber M and Zorn CN: Differential Lyn-dependence of the SHIP1-deficient mast cell phenotype. Cell Commun Signal 14: 12, 2016.
26. Lambertini E, Penolazzi L, Tavanti E, Schincaglia GP, Zennaro M, Gambari R and Piva R: Human estrogen receptor alpha gene is a target of Runx2 transcription factor in osteoblasts. Exp Cell Res 313: 1548-1560, 2007.
27. Lisignoli G, Lambertini E, Manferdini C, Gabusi E, Penolazzi L, Paolella F, Angelozzi M, Casagranda V and Piva R: Collagen type XV and the 'osteogenic status'. J Cell Mol Med 21: 2236-2244, 2017.
28. Livak KJ and Schmittgen TD: Analysis of relative gene expression data using real-time quantitative PCR and the 2(-Delta Delta C(T)) method. Methods 25: 402-408, 2001.
29. Penolazzi L, Lambertini E, Bergamin LS, Roncada T, De Bonis P, Cavallo M and Piva R: MicroRNA-221 silencing attenuates the degenerated phenotype of intervertebral disc cells. Aging (Albany NY) 10: 2001-2015, 2018.
30. Ma K, Chen S, Li Z, Deng X, Huang D, Xiong L and Shao Z: Mechanisms of endogenous repair failure during intervertebral disc degeneration. Osteoarthritis Cartilage 27: 41-48, 2019.
31. Lefebvre V and Dvir-Ginzberg M: SOX9 and the many facets of its regulation in the chondrocyte lineage. Connect Tissue Res 58: 2-14, 2017.
32. Alvarez-Garcia O, Matsuzaki T, Olmer M, Miyata K, Mokuda S, Sakai D, Masuda K, Asahara H and Lotz MK: FOXO are required for intervertebral disk homeostasis during aging and their deficiency promotes disk degeneration. Aging Cell 17: e12800, 2018.
33. Sivan SS, Hayes AJ, Wachtel E, Caterson B, Merkher Y, Maroudas A, Brown S and Roberts S: Biochemical composition and turnover of the extracellular matrix of the normal and degenerate intervertebral disc. Eur Spine J 23 (Suppl 3): S344-S353, 2014.
34. Liang H, Luo R, Li G, Zhang W, Song Y and Yang C: The proteolysis of ECM in intervertebral disc degeneration. Int J Mol Sci 23: 1715, 2022.
35. Dimozi A, Mavrogonatou E, Sklirou A and Kletsas D: Oxidative stress inhibits the proliferation, induces premature senescence and promotes a catabolic phenotype in human nucleus pulposus intervertebral disc cells. Eur Cell Mater 30: 89-102, 2015.
36. Wang X, Li H, Xu K, Zhu H, Peng Y, Liang A, Li C, Huang D and Ye W: SIRT1 expression is refractory to hypoxia and inflammatory cytokines in nucleus pulposus cells: Novel regulation by HIF-1α and NF-κB signaling. Cell Biol Int 40: 716-726, 2016.
37. Song Y, Lu S, Geng W, Feng X, Luo R, Li G and Yang C: Mitochondrial quality control in intervertebral disc degeneration. Exp Mol Med 53: 1124-1133, 2021.
38. Clouet J, Fusellier M, Camus A, Le Visage C and Guicheux J: Intervertebral disc regeneration: From cell therapy to the development of novel bioinspired endogenous repair strategies. Adv Drug Deliv Rev 146: 306-324, 2019.
39. Kaufmann T, Strasser A and Jost PJ: Fas death receptor signalling: Roles of Bid and XIAP. Cell Death Differ 19: 42-50, 2012.
40. Brown R: The bcl-2 family of proteins. Br Med Bull 53: 466-477, 1997.
41. Ciesielska S, Slezak-Prochazka I, Bil P and Rzeszowska-Wolny J: Micro RNAs in regulation of cellular redox homeostasis. Int J Mol Sci 22: 6022, 2021.
42. Lolli A, Narcisi R, Lambertini E, Penolazzi L, Angelozzi M, Kops N, Gasparini S, van Osch GJ and Piva R: Silencing of antichondrogenic MicroRNA-221 in human mesenchymal stem cells promotes cartilage repair in vivo. Stem Cells 34: 1801-1811, 2016.
43. Marques-Rocha JL, Samblas M, Milagro FI, Bressan J, Martínez JA and Marti A: Noncoding RNAs, cytokines, and inflammation-related diseases. FASEB J 29: 3595-3611, 2015.
44. Kang L, Zhang H, Jia C, Zhang R and Shen C: Targeting oxidative stress and inflammation in intervertebral disc degeneration: Therapeutic perspectives of phytochemicals. Front Pharmacol 13: 956355, 2022.
45. Roychoudhury S, Sinha B, Choudhury BP, Jha NK, Palit P, Kundu S, Mandal SC, Kolesarova A, Yousef MI, Ruokolainen J, *et al*: Scavenging properties of plant-derived natural biomolecule para-coumaric acid in the prevention of oxidative stress-induced diseases. Antioxidants (Basel) 10: 1205, 2021.
46. Ferreira PS, Victorelli FD, Fonseca-Santos B and Chorilli M: A review of analytical methods for p-coumaric acid in plant-based products, beverages, and biological matrices. Crit Rev Anal Chem 49: 21-31, 2019.
47. Kamali A, Ziadlou R, Lang G, Pfannkuche J, Cui S, Li Z, Richards RG, Alini M and Grad S: Small molecule-based treatment approaches for intervertebral disc degeneration: Current options and future directions. Theranostics 11: 27-47, 2021.
48. Saud B, Malla R and Shrestha K: A review on the effect of plant extract on mesenchymal stem cell proliferation and differentiation. Stem Cells Int 2019: 7513404, 2019.
49. Hori YS, Kuno A, Hosoda R and Horio Y: Regulation of FOXOs and p53 by SIRT1 modulators under oxidative stress. PLoS One 8: e73875, 2013.
50. Zhu H, Zhang L, Itoh K, Yamamoto M, Ross D, Trush MA, Zweier JL and Li Y: Nrf2 controls bone marrow stromal cell susceptibility to oxidative and electrophilic stress. Free Radic Biol Med 41: 132-143, 2006.
51. Dai X, Yan X, Wintergerst KA, Cai L, Keller BB and Tan Y: Nrf2: Redox and metabolic regulator of stem cell state and function. Trends Mol Med 26: 185-200, 2020.
52. Kubo Y, Beckmann R, Fragoulis A, Conrads C, Pavanram P, Nebelung S, Wolf M, Wruck CJ, Jahr H and Pufe T: Nrf2/ARE signaling directly regulates SOX9 to potentially alter age-dependent cartilage degeneration. Antioxidants (Basel) 11: 263, 2022.
53. Zhao S, Huang Z, Jiang H, Xiu J, Zhang L, Long Q, Yang Y, Yu L, Lu L and Gu H: Sirtuin 1 induces choroidal neovascularization and triggers age-related macular degeneration by promoting LCN2 through SOX9 deacetylation. Oxid Med Cell Longev 2022: 1671438, 2022.

54. de Crombrugghe B, Lefebvre V, Behringer RR, Bi W, Murakami S and Huang W: Transcriptional mechanisms of chondrocyte differentiation. Matrix Biol 19: 389-394, 2000.
55. Tan Z, Niu B, Tsang KY, Melhado IG, Ohba S, He X, Huang Y, Wang C, McMahon AP, Jauch R, *et al*: Synergistic co-regulation and competition by a SOX9-GLI-FOXA phasic transcriptional network coordinate chondrocyte differentiation transitions. PLoS Genet 14: e1007346, 2018.
56. Zhang CY, Hu XC, Zhang GZ, Liu MQ, Chen HW and Kang XW: Role of Nrf2 and HO-1 in intervertebral disc degeneration. Connect Tissue Res 63: 559-576, 2022.
57. Ganesh GV, Ganesan K, Xu B and Ramkumar KM: Nrf2 driven macrophage responses in diverse pathophysiological contexts: Disparate pieces from a shared molecular puzzle. Biofactors 48: 795-812, 2022.
58. Singh P, Gupta A, Qayoom I, Singh S and Kumar A: Orthobiologics with phytobioactive cues: A paradigm in bone regeneration. Biomed Pharmacother 130: 110754, 2020.
59. Wagner H and Ulrich-Merzenich G: Synergy research: Approaching a new generation of phytopharmaceuticals. Phytomedicine 16: 97-110, 2009.
60. Caesar LK and Cech NB: Synergy and antagonism in natural product extracts: When 1 + 1 does not equal 2. Nat Prod Rep 36: 869-888, 2019.